ANALYSIS OF DYNAMIC CHARACTERISTICS OF AN EXPERIMENTAL BENCH OF HIGH-PRESSURE WATER FRACTURING ASSISTED CUTTING

Zhiming Liu

School of Mechanical Electronic and Information Engineering, China University of Mining and Technology-Beijing, Beijing, China

Qiang Zhang, Yuliang Sun, Junming Liu

College of Mechanical and Electronic Engineering, Shandong University of Science and Technology, Tsingtao, China

Corresponding author Junming Liu, e-mail: junmingleo@163.com

Aiming at the problem that the cutting efficiency of a drum shearer is low when mining hard coal seams, an experimental bench of high-pressure water fracturing assisted cutting is designed. Compared with normal ones, the maximum equivalent stress of the improved experimental bench is reduced by 55.38%, and the maximum total deformation is reduced by 27.23%. According to the results of dynamic response analysis, it is concluded that the experimental bench of high-pressure water fracturing assisted cutting is stable and reliable under extreme working conditions, and meets design requirements for strength and stiffness.

Keywords: high-pressure water fracturing, experimental bench, dynamic characteristics

1. Introduction

Coal is the bottom-line guaranteed energy, and will continue to provide strong support for development of national economy and social stability. There is a large number of hard coal seam reserves in China's coal resources, and the conventional mechanical mining method has poor adaptability in the hard coal mining process (Zhang *et al.*, 2022b). How to realize safe and efficient mining of a hard coal seam is one of the research topics that has been widely concerned at present. Scholars at home and abroad search for an efficient method of mechanical cutting assisted by other means. In addition to traditional drilling and blasting, the current methods of coal breaking with assistance mainly include microwave irradiation assisted coal breaking (Hassani *et al.*, 2016), high pressure water jet assisted coal breaking (Liu, 2022b), impact pick assisted coal breaking (Zhang *et al.*, 2022a) and high-pressure water fracturing assisted coal breaking (Jiang *et al.*, 2012; Li *et al.*, 2021).

Teimoori and Cooper (2021) developed and analyzed numerical simulation of rock-microwave interaction via the finite element method to solve the electric field and magnetic field, temperature distribution and maximum principal stress. The results showed that microwave energy has potential application prospects for rock fragmentation and continuous excavation. Wang *et al.* (2021) proposed a shearer drum with an abrasive slurry jet, and studied the effects of multiple parameters on the rock-breaking ability of the abrasive slurry jet combined with picks through orthogonal experiments. Cui *et al.* (2022) studied breaking characteristics of rock samples with size of 700 mm×700 mm×700 mm by using a high-pressure foam fracturing device. The effects of well depth, seal length and foam pressure were analyzed. The results showed that when the well depth was 100-120 mm, the sealing length was 30-10 mm, and the foam pressure was 15-16.5 MPa, the rock failure mode changed from blasting pit to stripped boulder. Deng *et al.* (2022) created a physical model using rectangular and circular laser points to scan the broken

rock, and verified the accuracy of the model through a combination of experiments and numerical simulations. Li *et al.* (2021) used a hydraulic fracturing system and simulated the cutting system to cut rock samples after fracturing, and found that the cutting torque and cutting resistance were significantly reduced after fracturing. Liu *et al.* (2022a) used ASJ method to study the effect of mud properties and working parameters on rock cutting performance, and analyzed the rock cutting resistance and specific energy (SE) of ASJ-assisted conical pick. Xi *et al.* (2022) conducted orthogonal experiments of the split Hopkinson pressure bar (SHPB) device to analyze 13 parameters of the Riedel Hiermaier Thoma (RHT) material model, considering the actual size of drilling teeth and the load transmitted to the formation. Subsequently, the numerical simulation results of the SHPB test and cutting experiment were verified using a physical model. Zhang *et al.* (2022b) considered the combination of impact action and cutting action, and studied cutting characteristics of the impact pick by combining theoretical analysis, numerical simulation and an experiment. Zhao *et al.* (2021) proposed a finite element numerical modeling method for a dynamic cutting process under different ultra-high pressure loads. The cutting force, mechanical specific energy (MSE), rock failure mode and crack propagation process of heterogeneous rock with natural cracks were analyzed and compared with cutting conditions under a steady load. Deng *et al.* (2004) summarized the hydraulic fracturing mechanism of a hard coal seam through theoretical analysis and engineering practice, that is, injecting high-pressure water into the coal seam to produce cracks and weaken strength of the coal body and improve the cutting efficiency.

Among the above various methods of coal breaking with assistances, the method of high pressure water fracturing assisted cutting has broad application prospects. At present, the experimental research in the method of high-pressure water fracturing assisted cutting is mostly focused on the engineering field, and experimental devices in the related fields are mostly water jet experimental benches. There is a lack, however, an experimental device of high-pressure water fracturing assisted cutting in the laboratory. Therefore, this paper designs an experimental bench of high-pressure water fracturing assisted cutting and analyzes its structural dynamic response characteristics, which can provide a reliable experimental platform for relevant experiments.

2. Principle of the experimental bench of high-pressure water fracturing assisted cutting and a finite element model establishment

2.1. Composition and principle of the experimental bench

The structure of the experimental bench of high-pressure water fracturing assisted cutting is mainly composed of the main frame, traction slide table, propulsion slide table, mounting plate for samples, cutting drum, device for confining pressure loading and device of high-pressure water fracturing, as shown in Fig. 1.

The propulsion slide table is connected with the frame, traction slide table and the propulsion slide table through linear guide rails. Ball screw pairs are respectively installed between the propulsion slide table and the frame, and between the traction slide table and the propulsion slide table, which are driven by their respective connected servo motors. A motor for controlling the cutting drum, a reducer, speed and torque sensor, bearing seats and the cutting drum are successively installed on the traction slide table. The input and output ends of the speed and torque sensors are connected with the front and rear shafts by the internal tooth coupling, and picks are installed on the cutting drum.

The top hydraulic cylinder and side hydraulic cylinder are installed on the mounting plate. The piston rod of each hydraulic cylinder is connected with a pressing plate. When the piston rod extends, the pressure plate will apply pressure to the sample in order to simulate the confining pressure of deep coal and rock. A water tank is placed under the mounting plate to provide
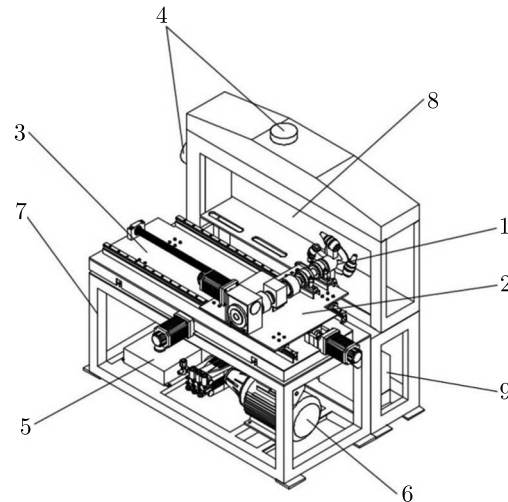
Fig. 1. Structural diagram of experimental bench of high-pressure water fracturing assisted cutting:
1 – cutting drum, 2 – traction slide table, 3 – propulsion slide table, 4 – hydraulic cylinder, 5 – hydraulic oil tank, 6 – high pressure pump, 7 – main frame, 8 – mounting plate for samples, 9 – water tank

water source for fracturing. The oil tank is installed under the main frame to provide power for the confining pressure loading device. A high-pressure pump is installed under the main frame to generate high-pressure water flow for fracturing.

The working principle of the experimental bench is as follows: Place the specimens on the mounting plate, turn on the hydraulic loading device, and apply pressure to the top and side walls of the specimens. Then start the high-pressure water pump, inject the high-pressure water into the specimens through the pipeline, and seal the water injection hole with a hole sealer. Micro cracks are generated in the specimen and then they will propagate and penetrate until the final macro cracks are generated, which leads to instability and fracture of the specimen. After the specimen is fractured by high-pressure water, the drum starts to cut it.

2.2. Establishment of the finite element model of the experimental bench

The experimental bench of high-pressure water fracturing assisted cutting studied in this paper is an assembly in which there are many connection relations between various parts. The constituent parts of the experimental bench contain many threaded holes, rounded corners and chamfers. If the finite element model is created completely according to the actual situation, it will be very complex and occupy a lot of memory resources in the calculation process. So these detail features need to be simplified. The mounting plate is not directly connected with the cutting part. This paper mainly analyzes the dynamic response of the experimental bench except for the mounting plate. Retaining the structure with large mass on the experimental bench has a great impact on the dynamic characteristics. SolidWorks is used for modeling the simplified three-dimensional experimental bench of high-pressure water fracturing assisted cutting, as shown in Fig. 2.

The simplified three-dimensional model is imported into ANSYS Workbench to establish the finite element model of the experimental bench. According to the Chinese standard of steel classification, the materials of the experimental bench mainly include aluminum alloy, cast iron and steel grades GCr15, GCr 45, 42CrMo and 40Cr, respectively. The material of the main frame, propulsion slide table and traction slide table are 40Cr steel. The material of lead screws, guide rails, nuts and sliding block is GCr15 steel. The material of nut seats, internal tooth coupling, cutting drum and main shaft is 45 steel. The material of the casing of the reducer and speed torque sensor is aluminum alloy. The material of picks, pick sleeves and pick seats is 42CrMo
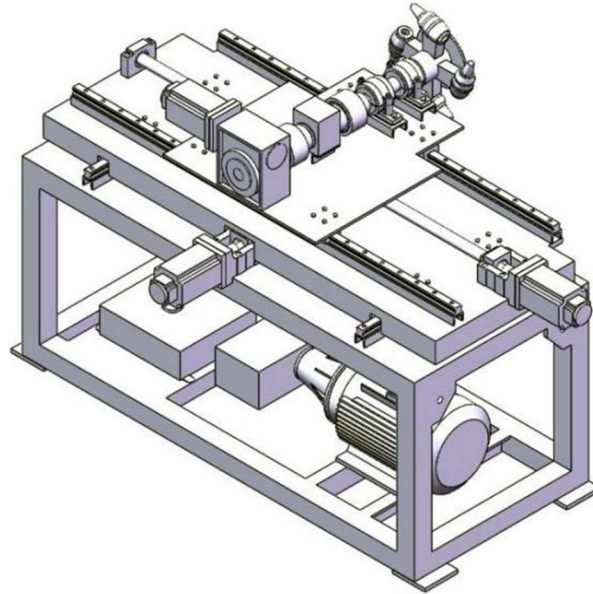
Fig. 2. Simplified three-dimensional model of the experimental bench

steel. And the material of keys, bolts, nuts and other parts installed on the experimental bench is 45 steel. The parameter settings of each material in the finite element model of the experimental bench are shown in Table 1.

Table 1. Parameters of each material in the finite element model of the experimental bench

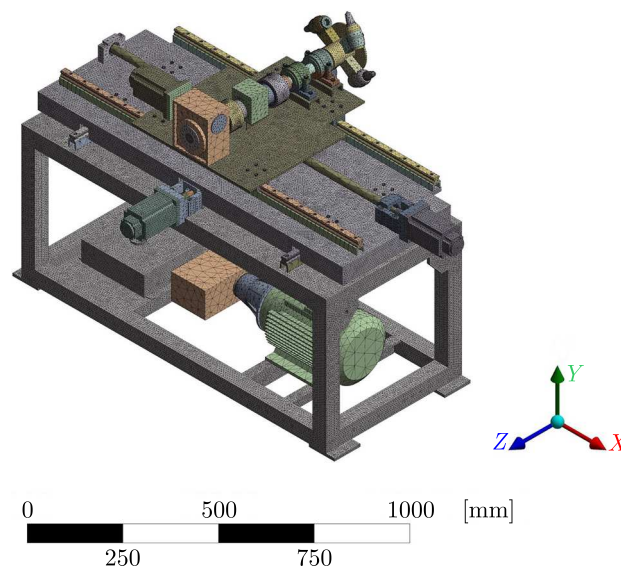| Material type	Poisson's ratio	Density [kg/m^3]	Young's modulus [MPa]
GCR15	0.30	7810	2.08E+5
45 steel	0.27	7850	2.00E+5
42CrMo	0.28	7850	2.12E+5
40Cr	0.30	7850	2.10E+5
Aluminum alloy	0.33	2700	7.00E+4

Fig. 3. Finite element model of the experimental bench

As shown in Fig. 3, after the three-dimensional model is established, it is meshed and constrained. The mesh type is selected as a tetrahedron, and the value of relevance is set to 20. The result of meshing is 1,026,377 elements. The constraint type of the contact plane between the bottom of the experimental bench and the ground is set as fixed contact. Other components such as the motor and guide rail are fixed to the experimental bench through bolts, and the contact surface type is bound contact. The rotation constraint is used for rotating components such as the cutting head.

3. Dynamic characteristics analysis of the experimental bench of high-pressure water fracturing assisted cutting

3.1. Modal analysis of the experimental bench

According to Newton's second law, motion of the experimental bench of high-pressure water fracturing assisted cutting can be expressed by a linear differential equation as

$$\mathbf{M}\ddot{\mathbf{X}}(t) + \mathbf{C}\dot{\mathbf{X}}(t) + \mathbf{K}\mathbf{X}(t) = \mathbf{F}(t) \tag{3.1}$$

where $\mathbf{M}$ is the mass matrix, $\mathbf{C}$ – damping matrix, $\mathbf{K}$ – stiffness matrix of the experimental bench, $\ddot{\mathbf{X}}(t)$ is the acceleration vector, $\dot{\mathbf{X}}(t)$ – velocity vector, $\mathbf{X}(t)$ – displacement vector, $\mathbf{F}(t)$ is the external excitation vector.

In order to determine the natural frequency and vibration mode of the experimental bench, an undamped homogeneous vibration equation of the system can be obtained by simplifying equation (3.1), that is

$$\mathbf{M}\ddot{\mathbf{X}}(t) + \mathbf{K}\mathbf{X}(t) = \mathbf{0} \tag{3.2}$$

Due to the fact that the elastic body can be decomposed into a series of simple harmonic vibrations under the state of free vibration, the solution of the equation is

$$\mathbf{X}(t) = x\mathrm{e}^{\mathrm{j}\omega t} \tag{3.3}$$

where ω is the angular frequency.

Substitute equation (3.3) and its second derivative into equation (3.2), the equation is obtained as

$$(\mathbf{K} - w^2\mathbf{M})(x)\mathrm{e}^{\mathrm{j}\omega t} = \mathbf{0} \tag{3.4}$$

Equation (2.4) is a homogeneous algebraic equation about $\mathbf{x}$ of w^2, and the only condition for this equation to have a non-zero solution is that its coefficient determinant is zero, that is

$$|\mathbf{K} - w^2\mathbf{M}| = 0 \tag{3.5}$$

or

$$d_{2n}w^2 + d_{2n-2}w^{2n-2} + \cdots + d_0 = 0 \tag{3.6}$$

The above formula is the n-th order polynomial of w^2 containing coefficients of the characteristic equation or frequency equation $d_{2n}, d_{2n-2}, \ldots, d_0$. The roots $w_1^2, w_2^2, w_3^2, \ldots, w_n^2$ of the characteristic equation are the only n eigenvalues to ensure that hypothetical solution (3.3) can be found, and its square root is the undamped natural frequency of the vibration system. Substituting any natural frequency into equation (3.4), a value corresponding to the phase $\mathbf{x}$ of the amplitude

vector can be obtained, which represents the eigenvalue of the natural frequency. And deformation characteristics of the discrete mass in the vibration equation under the corresponding natural frequency are determined.

Modal analysis can help designers to determine the natural frequency and mode shape of the structure, so as to avoid a resonance and predict the vibration mode of the structure under different loads. The experimental bench of high-pressure water fracturing assisted cutting will vibrate under the influence of an external excitation in the working process. When the external excitation frequency is close to the natural frequency of a certain order, the experimental bench may resonate and affect its stability and performance.

In order to avoid the harm for resonance, it is necessary to carry out modal analysis. The first 8 order modes are extracted in this modal analysis, and the first 8 order natural frequencies of the experimental bench are obtained after solving, as shown in Table 2. The first 8 modal shapes are extracted as shown in Fig. 4.

Table 2. The first 8 order natural frequencies of the experimental bench

Modal order	Natural frequency [Hz]	Modal order	Natural frequency [Hz]
1	34.718	5	64.318
2	40.816	6	71.821
3	50.803	7	90.130
4	56.064	8	95.295

In Fig. 4, it can be seen that the first order mode shapes show a right inclination of the upper part of the bench. The second shows a deformation of the traction unit and cutting unit. The third and the fourth show an upward deformation on the bottom of the main frame and the pump as well as the drum, respectively. The fifth and the seventh show a right inclination of the reducer and the motors. The sixth shows a torsional deformation of the bench and the eighth one shows an upward deformation on the bottom of the main frame and the pump.

In the process of cutting, the excitation frequency of the cutting force not only acts on the part for mechanical cutting, but also on the mounting plate through specimen conduction. It is also necessary to conduct modal analysis of the mounting plate. The mounting plate is not directly connected with the part for mechanical cutting, so the modal analysis is carried out separately. In this modal analysis, the material of the mounting plate is 45 steel, and the grid element size is set as 5 mm. A total of 1414169 elements are obtained, and fixed constraints are added at the bottom of the frame. The first 8 order natural frequencies of the mounting plate are obtained, as shown in Table 3.

Table 3. The first 8 natural frequencies of the mounting plate

Modal order	Natural frequency [Hz]	Modal order	Natural frequency [Hz]
1	26.576	5	102.62
2	35.299	6	127.35
3	57.191	7	137.86
4	95.391	8	156.16

During the high-pressure water fracturing stage of the experiment, the source of the excitation frequency is mainly the motor driving the high-pressure pump. The working speed of the motor is 1450 r/min, and the excitation frequency is 24.17 Hz. It will not have a great impact on the structure of the experimental bench, and it will not resonate.

During the cutting stage of the experiment, the excitation frequency mainly comes from two parts. One of them comes from rotational motion of the parts installed in the experimental bench. The maximum working speed of the motor controlling the cutting speed is 2000 r/min,
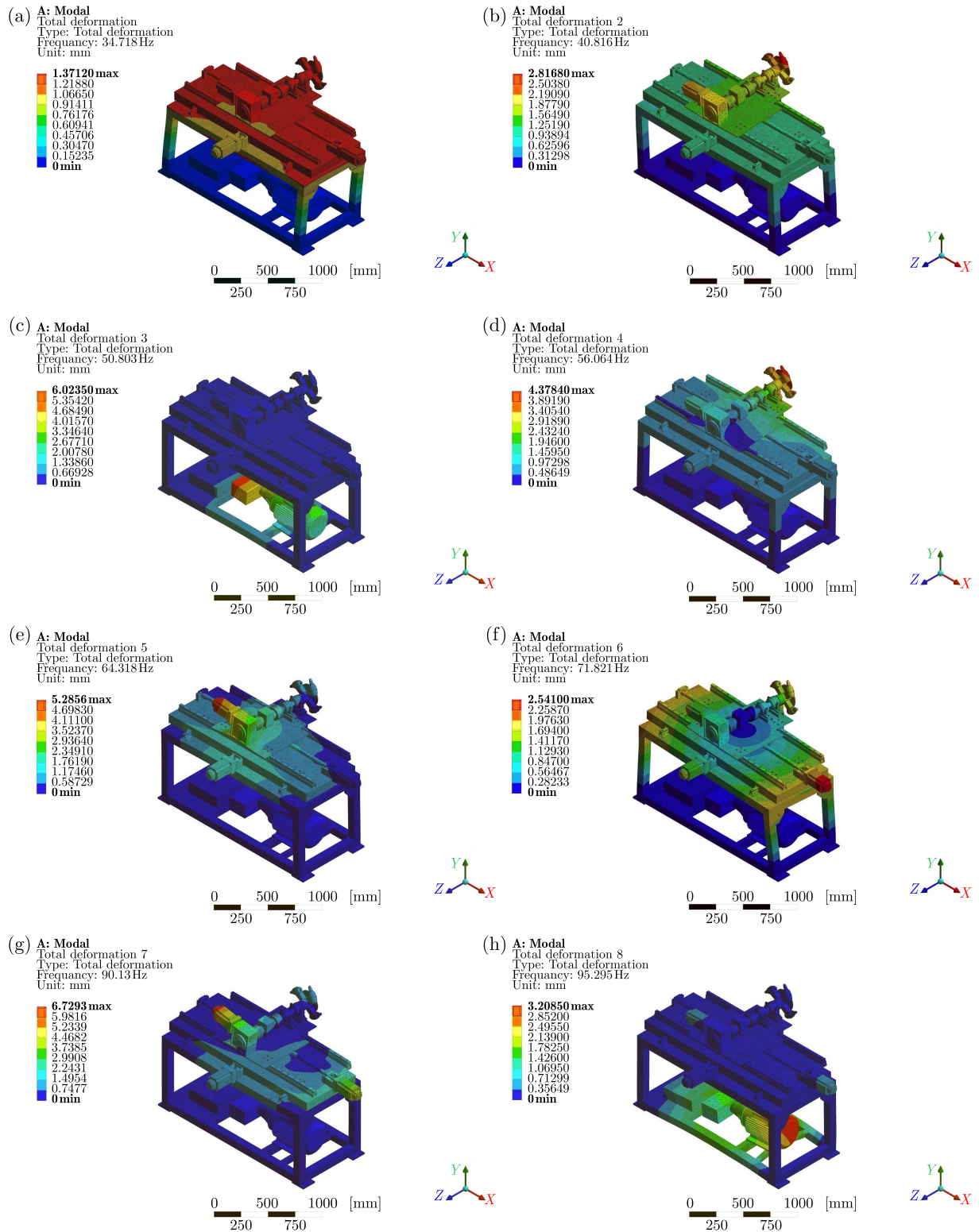
Fig. 4. First 8 order mode shapes of the experimental bench: (a) first order mode shapes, (b) second order mode shapes, (c) third order mode shapes, (d) fourth order mode shapes, (e) fifth order mode shapes, (f) sixth order mode shapes, (g) seventh order mode shapes, (h) eighth order mode shapes

and the excitation frequency is 33.33 Hz; the maximum working speed of the cutting drum and the main shaft is 41.67 r/min, and the excitation frequency is 0.69 Hz; the maximum working speed of the servo motor and lead screw in the traction sliding assembly is 1200 r/min, and the excitation frequency is 20 Hz; the maximum working speed of the servo motor and lead screw in the propulsion sliding assembly is 1500 r/min, and the excitation frequency is 25 Hz.

Another part of the excitation frequency comes from the influence of the cutting force excitation on the drum in the process of cutting. The dominant frequency of the cutting force is concentrated in a low order. It is further inferred that in the normal cutting experiment, the structure of the experimental bench of high-pressure water fracturing assisted cutting designed in this paper will not resonate due to the excitation of the load on the drum. Comparing the natural frequency and external excitation frequency of the experimental bench, the excitation frequency of the cutting motor is close to the first-order natural frequency, which may affect the structure of the experimental bench.

3.2. Harmonic response analysis of the experimental bench

The harmonic response analysis can find the steady-state response of the system under different frequency harmonic loads. In order to accurately judge the low-order resonance frequency range of the experimental bench, the harmonic response analysis is carried out. Based on the results of modal analysis, the modal superposition method is used to analyze the harmonic response of the experimental bench. The frequency range is set up between 0-120 Hz, the number of solution steps is 120, and 1000 N is applied in the X and Y direction and 500 N in the Z direction on the drum to solve the harmonic response of the experimental bench.

Through the first 8 order modes of the experimental bench, it can be found that the main frame, traction slide table and propulsion slide table are prone to large vibration. The traction slide table, propulsion slide table and main frame are selected as the research object, and the vibration amplitude-frequency response curves of are obtained, as shown in Fig. 5 and Fig. 6, respectively.
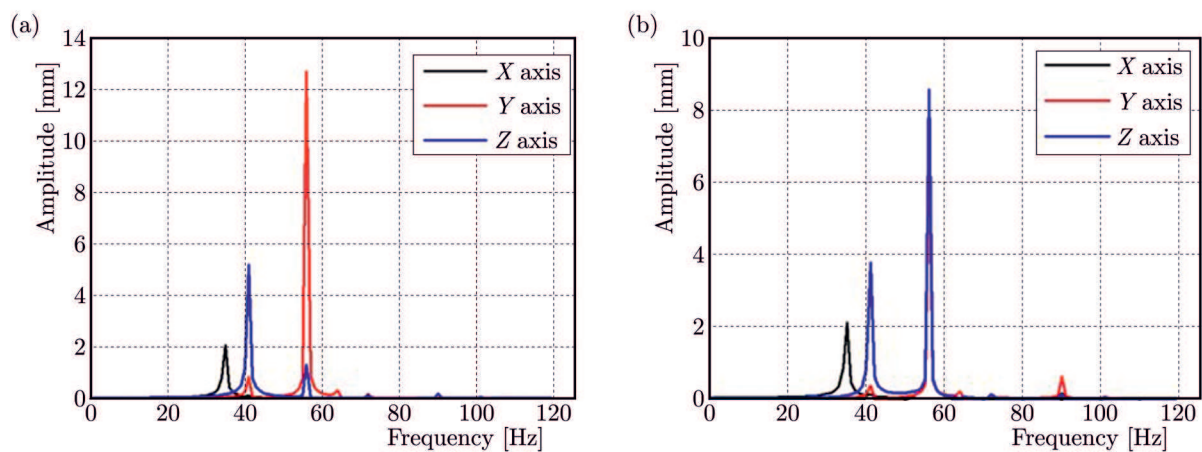

Fig. 5. Amplitude frequency response curves of: (a) traction slide table, (b) propulsion slide table

It can be seen from Fig. 5a that under the action of external loads, the amplitude peaks of the traction slide table along the X-axis, Y-axis and Z-axis appear at 35 Hz, 56 Hz and 41 Hz, respectively, and the maximum values are 2.103 mm, 12.754 mm and 5.221 mm, respectively. And it can be seen from Fig. 5b that the amplitude peaks of the propulsion slide table along the X-axis, Y-axis and Z-axis appear at 35 Hz, 56 Hz and 56 Hz, respectively, and the maximum values are 2.126 mm, 7.043 mm and 8.580 mm, respectively.
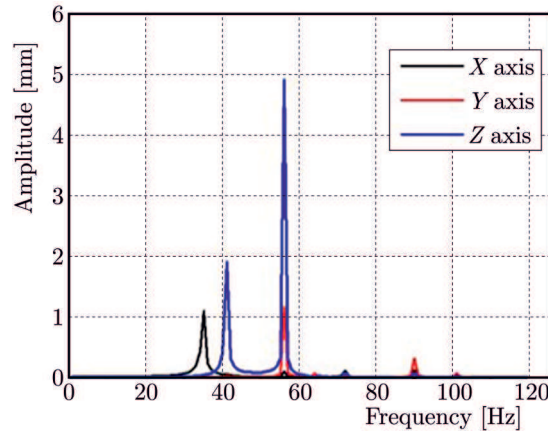
Fig. 6. Amplitude frequency response curves of the main frame

It can be seen from Fig. 7 that the amplitude peaks of the main frame along the X-axis, Y-axis and Z-axis appear at 35 Hz, 56 Hz and 56 Hz, respectively, and the maximum values are 1.114 mm, 1.167 mm and 4.918 mm, respectively.

Through the analysis of the amplitude-frequency response curves of the traction slide table, propulsion slide table and main frame along the X, Y and Z axis combined with the current operation of the experimental bench, it can be concluded that the experimental bench is prone to resonate under the action of force whose excitation frequency is close to its first-order natural frequency. Subsequent improvements to the structure of the experimental bench are required to increase its low-order natural frequency.

3.3. Transient dynamic analysis of the experimental bench

In this paper, the load spectrum of the experimental bench of high-pressure water fracturing assisted cutting under extreme working conditions is selected as the applied load, that is, the drum cuts the specimen without high-pressure water fracturing. At this time, the loads on the experimental bench are large and have a great impact on the structure. Before transient dynamic analysis, the drum cutting model of the experimental bench is established by EDEM, and the load spectrum of the experimental bench under extreme working conditions is obtained.

In this paper, the Hertz-Mindlin with bonding contact model is used to simulate the cutting process of coal and rock. Since there is no uniform standard in the parameter setting of the bond between particles, it is mostly estimated by empirical formulas

$$k_n = \frac{4}{3}\Big(\frac{2(1-\nu^2)}{E}\Big)^{-1}\Big(\frac{2}{r}\Big)^{-\frac{1}{2}} \qquad k_s = \Big(\frac{1}{2} \sim \frac{2}{3}\Big)k_n \qquad \tau = C + \sigma \tan\varphi \qquad (3.7)$$

where k_n and k_s is the normal stiffness and tangential stiffness coefficient [N/m^2], r is the particle radius [m], ν is Poisson's ratio, E is the elastic modulus, σ is the normal limit stress [Pa], τ is the tangential limit stress [Pa], φ is the internal friction angle [°], C is cohesion [Pa].

The parameters used in the simulation are: (1) The shear modulus of materials of the cutting drum and coal wall are 70 GPa and 1.72 GPa, respectively, Poisson's ratio is 0.31 and 0.2, respectively, and density is 7850 kg/m^3 and 1325 kg/m^3, respectively; (2) The particles forming the coal wall are spherical particles with a radius of 10 mm. The static friction coefficient, dynamic friction coefficient and recovery coefficient between the drum and the coal wall are 0.45, 0.08 and 0.35, respectively. And the static friction coefficient, dynamic friction coefficient and recovery coefficient between the coal wall particles are 0.5, 0.2 and 0.5, respectively; (3) The contact model between particles is Hertz-Mindlin's with bonding, the contact model between the coal wall particles and drum is Hertz-Mindlin's (no slip) during cutting process.

According to the simulation results of the discrete element model, the load spectrum of the experimental bench under extreme working conditions is obtained. A group of data near the peak point of the cutting force curve is selected as the external load in the transient analysis. Specifically, the load applied to the cutting drum in this transient dynamic analysis is shown in Fig. 7. The drum is under a discrete impact condition during cutting. At the rated speed, a single pick only contacts the coal wall once per circle. According to the speed setting of the experimental bench, the paper mainly focuses on the limit load of a single pick. In order to save simulation time and improve simulation efficiency, the total simulation time is set to 0.2 s, which is divided into 40 substeps.
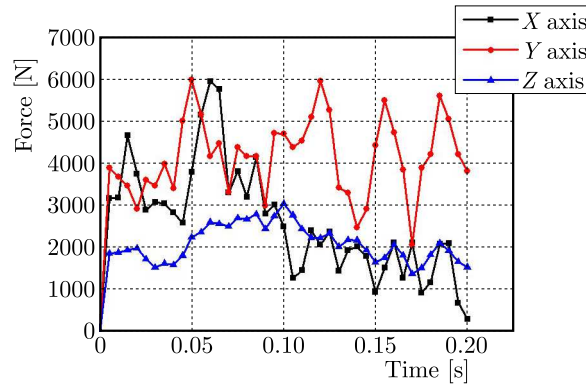

Fig. 7. Loads in transient dynamic analysis

A chance in time of the load applied to the pick tip is taken into account and a fixed constraint at the bottom of the experimental bench is added. The drum speed is set to 4.356 rad/s, and the linear speed of the traction slide is 60 mm/s. Static analysis of the experimental bench after loading is carried out, and the equivalent stress curve and total deformation curve are shown in Fig. 8.
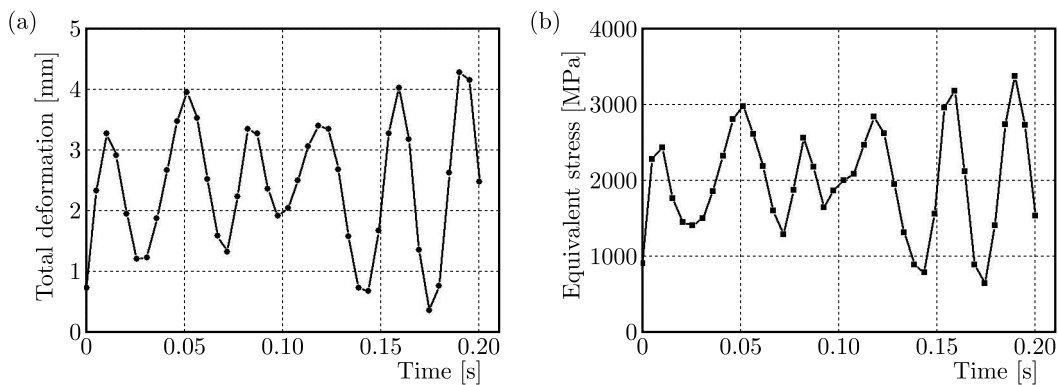

Fig. 8. The curve of (a) total deformation and (b) equivalent stress of the experimental bench with time

The maximum equivalent stress and total deformation of the experimental bench appears at 0.19 s. The equivalent stress distribution map and total deformation distribution map of the experimental bench at 0.19 s are extracted, as shown in Fig. 9.

According to Fig. 9, under the condition of time-varying loading force, the maximum equivalent stress and maximum deformation of the test bench are 335.7 MPa and 4.2659 mm, respectively. The equivalent stress and total deformation of the experimental bench in the process of cutting are large. It is necessary to improve the structure of the parts with large deformation and stress.
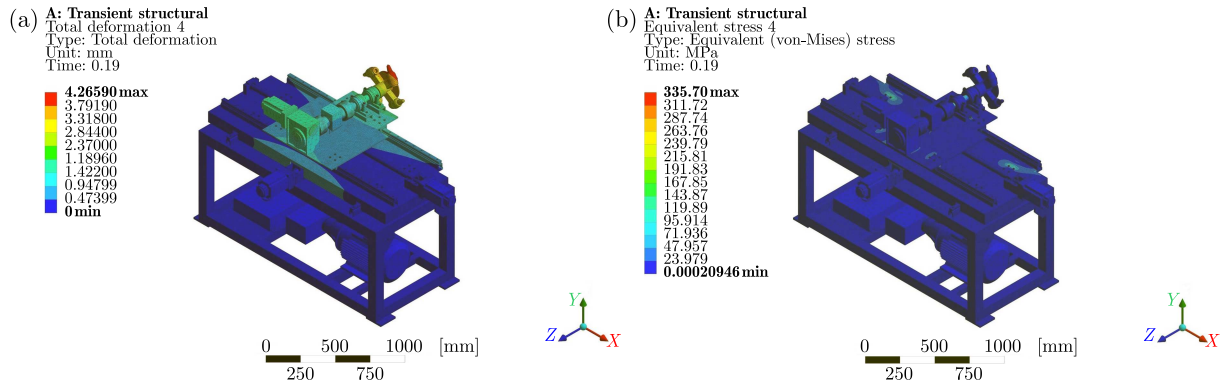
Fig. 9. Distribution nephogram of (a) total deformation and (b) equivalent stress of the experimental bench

3.4. Structural improvement of the experimental bench

According to the results of modal analysis of the traction sliding table, propulsion sliding table and frame, the vibration of the traction sliding table and propulsion sliding table is relatively large, and the low order natural frequency of the main frame has a great impact on the overall low order natural frequency of the whole experimental bench. It is necessary to optimize the structure of the experimental bench, enhance its overall natural frequency and reduce its equivalent stress and total deformation.

The experimental bench of high-pressure water fracturing assisted cutting is improved by increasing thickness of the steel plate of the support leg of the rack, and adding different forms of stiffeners at the bottom of the traction sliding table and the propulsion sliding table. The improved traction and propulsion slides are modeled using SolidWorks, as shown in Fig. 10.
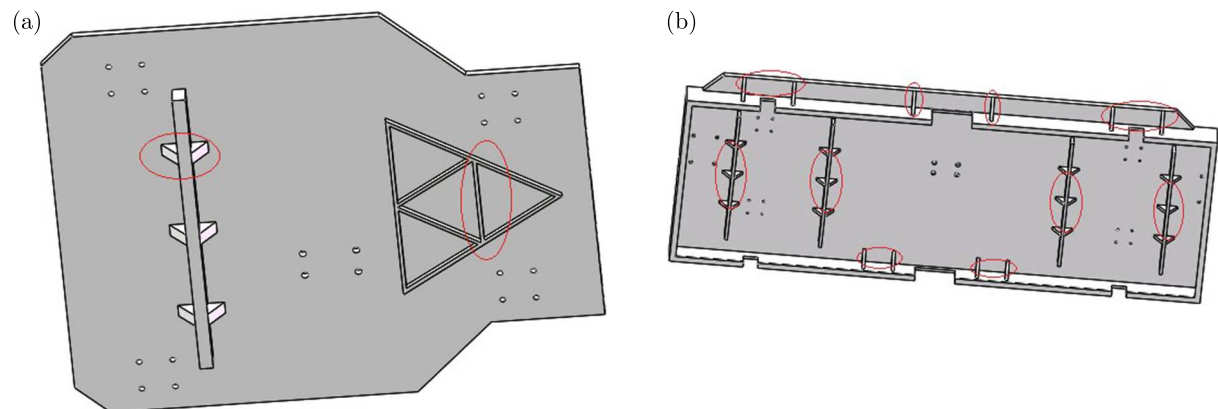

Fig. 10. Structure of the traction slide table and propulsion slide table after structural improvement: (a) traction slide table after improvement, (b) propulsion slide table after improvement

The modal analysis of the improved experimental bench is finished first, and the settings are the same as those before structural improvement. The first 8 order modes of the improved experimental bench are found. The first two order vibration modes have no obvious changes, but the vibration amplitude is reduced. After the structural improvement, the first 8 order natural frequencies are all increased. Among them, the first and second order natural frequencies are 41.066 Hz and 46.642 Hz, respectively, which are increased by 18.28% and 14.27%, respectively. The first and second order natural frequencies are greater than the external excitation frequency of the experimental bench after structural improvement, which reduces the possibility of resonance of the experimental bench.

Then, the transient dynamical analysis of the improved experimental bench is finished, and the settings of simulation are the same as those before structural improvement. The simulation results are obtained via ANSYS Workbench, and the comparison curve of the total deformation and equivalent stress changing with time before and after the structural improvement is drawn, as shown in Fig. 11.
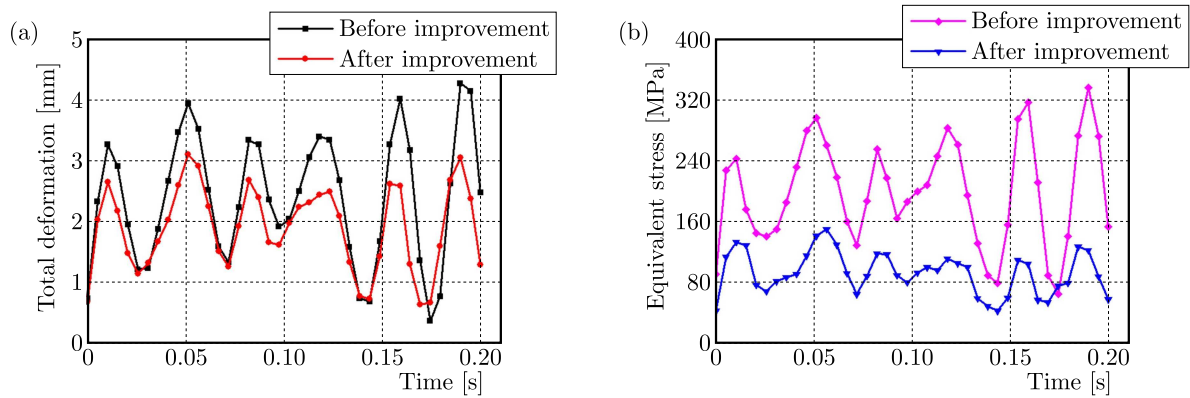

Fig. 11. Comparison diagram of (a) total deformation and (b) equivalent stress change curve before and after structural improvement of the experimental bench

It can be seen from the curves of total deformation before and after improvement in Fig. 11 that the amplitude of total deformation decreases as a whole after the structural improvement. From the curves of equivalent stress before and after the improvement, it is determined that the amplitude of equivalent stress after the improvement is greatly reduced compared with that before the improvement.
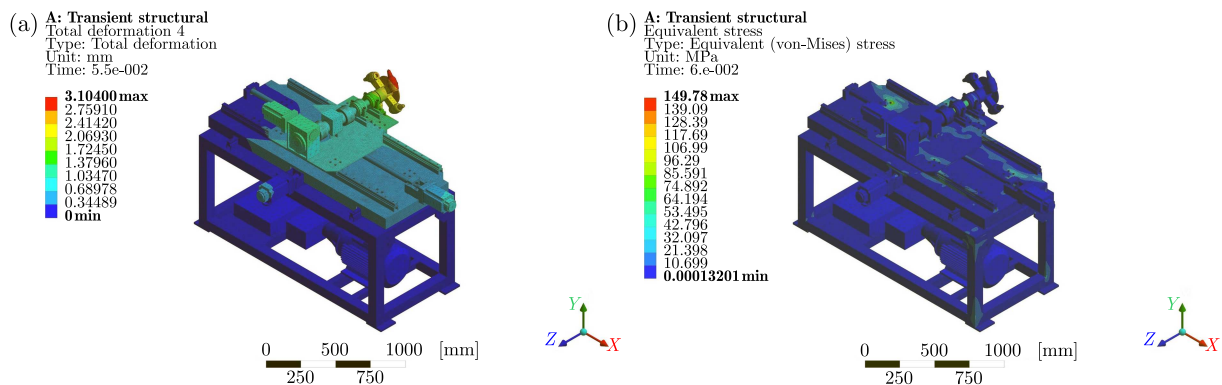

Fig. 12. Distribution nephogram of (a) maximum total deformation and (b) maximum equivalent stress of the experimental bench after structural improvement

The maximum total deformation nephogram and the maximum equivalent stress nephogram of the experimental bench after structural improvement are extracted, as shown in Fig. 12. The maximum equivalent stress after improvement is 149.78 MPa, 55.38% lower than that before improvement, which is lower than the allowable stress of its own material. The maximum total deformation of the improved experimental bench is 3.104 mm, which is 27.23% lower than that before the improvement. The overall stress distribution and deformation of the experimental bench have been greatly improved.

4. Discussion

The research presented in this article has some limitations. The damping effect is not discussed at all. In most dynamic problems (including linear dynamics and nonlinear dynamics), it is really important to define damping, but damping algorithms and parameters only approximate energy absorption characteristics of a structure. In this paper, the purpose of modal analysis is to find out the natural frequency rather than the amplitude of the structure. The purpose of transient dynamic analysis is to determine mechanical properties of the structure. It has been shown in previous studies that damping has little influence on the results of structural modal calculation and mechanical analysis, and it is very difficult to determine damping data in finite element calculation, so damping is not considered in the finite element calculation. In the future research work, we will continue to study the reliability of the experimental bench under some extreme conditions, and combine with the experimental verification. On the whole, the results indicate that the experimental bench of high-pressure water fracturing assisted cutting studied in this paper can be used as a reliable platform for carrying out experiments of high-pressure water fracturing assisted cutting, and provides a reference for the design and improvement of related experimental devices.

5. Conclusion

- In view of the lack of experimental equipment for high-pressure fracturing combined with cutting, an experimental bench of high-pressure water fracturing assisted cutting is designed. The main structure and principle are introduced, the finite element model of the experimental bench is established, and the dynamic characteristics of the experimental bench are analyzed based on the finite element method.
- The finite element model of the experimental bench is established. The first 8 order natural frequencies and modal shapes of the experimental bench are obtained in the modal analysis, and the external excitation frequencies of the experimental bench are analyzed. The results show that the excitation frequency of the cutting motor is 33.33 Hz, which is close to the first order natural frequency of 34.718 Hz, and may cause resonance. In the harmonic response analysis, the amplitude and frequency response curves of the traction slide table, the propulsion slide table and the main frame are obtained, and it is concluded that the excitation frequency that may cause the experimental bench to generate large vibration has multiple orders. However, the experimental bench is only prone to resonance at the excitation frequency close to its first order natural frequency when butting, which verifies the results of the modal analysis.
- In the transient dynamic analysis, the maximum equivalent stress of the experimental bench under the load spectrum in extreme working conditions is 335.7 MPa, and the maximum deformation is 4.2659 mm. The structure of the traction slide table, propulsion slide table and main frame are improved, and the modal analysis and transient dynamic analysis of the improved experimental bench are carried out. Compared with the experimental bench before improving, the first two order natural frequencies of the improved experimental bench increased by 18.28% and 14.27%, respectively. The overall maximum equivalent stress of the improved experimental bench is reduced by 55.38%, and the maximum deformation is reduced by 27.23%. The overall improvement effect of the experimental bench is remarkable.

References

1. Cui M., Zhai Y.H., Ji G.D., 2011, Experimental study of rock breaking effect of steel particles, *Journal of Hydrodynamics, Ser. B*, **23**, 2, 241-246

2. Cui S., Liu S.Y., Li H.S., Zhou F.Y., Sun D., 2022, Critical parameters investigation of rock breaking by high-pressure foam fracturing method, *Energy*, **258**, 124871

3. Deng G.Z., Wang S.B., Huang B.X., 2004, Research on behavior character of crack development induced by hydraulic fracturing in coal-rock mass (in Chinese), *Chinese Journal of Rock Mechanics and Engineering*, **23**, 20, 3489-3493

4. Deng R., Liu J.P., Kang M.Q., Zhang W., 2022, Simulation and experimental research of laser scanning breaking granite, *Optics Communications*, **502**, 127403

5. Hassani F., Nekoovaght P.M., Gharib N., 2016, The influence of microwave irradiation on rocks for microwave-assisted underground excavation, *Journal of Rock Mechanics and Geotechnical Engineering*, **8**, 1, 1-15

6. Jiang Z.M., Feng S.R., Fu S., 2012, Coupled hydro-mechanical effect of a fractured rock mass under high water pressure, *Journal of Rock Mechanics and Geotechnical Engineering*, **4**, 1, 88-96

7. Li H.S., Liu S.Y., Zhu Z.C., Liu H., Zhang D., Guo C., 2021, Experimental investigation on rock breaking performance of cutter assisted with hydraulic fracturing, *Engineering Fracture Mechanics*, **248**, 107710

8. Liu S.Y., Cui S., Li H.S., Zhou F., Xu B., Hu Y., 2022a, Impact characteristics of rock breaking using a conical pick assisted with abrasive slurry jet, *Engineering Fracture Mechanics*, **271**, 108647

9. Liu Z.H., Ma Z.K., Liu K., Zhao S., Wang Y., 2022b, Coupled CEL-FDEM modeling of rock failure induced by high-pressure water jet, *Engineering Fracture Mechanics*, **277**, 108958

10. Teimoori K., Cooper R., 2021, Multiphysics study of microwave irradiation effects on rock breakage system, *International Journal of Rock Mechanics and Mining Sciences*, **140**, 104586

11. Wang F.C., Li L.C., Zhou X., Lin J., Guo C.W., 2021, New application of abrasive slurry jet in coal rocks breaking and prediction model of its rock breaking ability, *Arabian Journal for Science and Engineering*, **46**, 8, 7227-7237

12. Xi Y., Wang W., Fan L.F., Zha C.Q., Li J., Liu G.H., 2022, Experimental and numerical investigations on rock-breaking mechanism of rotary percussion drilling with a single PDC cutter, *Journal of Petroleum Science and Engineering*, **208**, Part B, 109227

13. Zhang Q., Wang C., Tian Y., 2022a, Numerical and experimental study on crushing properties of hard coal using impacting-cutting technique, *Shock and Vibration*, **2022**, 7091553

14. Zhang Q., Wang C., Tian Y., 2022b, Study on shearer drum structure design and coal-breaking performance based on multi-impact picks for hard coal, *Environmental Earth Sciences*, **81**, 7, 189

15. Zhao Y., Zhang C.S., Zhang Z.Z., Gao K., Li J.S., Xie X.B., 2021, The rock breaking mechanism analysis of axial ultra-high frequency vibration assisted drilling by single PDC cutter, *Journal of Petroleum Science and Engineering*, **205**, 108859